Ocean Sci. Discuss., 6, 2357–2388, 2009
www.ocean-sci-discuss.net/6/2357/2009/
© Author(s) 2009. This work is distributed under
the Creative Commons Attribution 3.0 License.

Ocean Science Discussions

Papers published in *Ocean Science Discussions* are under
open-access review for the journal *Ocean Science*

Volume, heat, and freshwater fluxes towards the Arctic from combined altimetry and hydrography in the Norwegian Sea

K. A. Mork and Ø. Skagseth

Institute of Marine Research and Bjerknes Centre for Climate Research, Bergen, Norway

Received: 10 August 2009 – Accepted: 12 October 2009 – Published: 21 October 2009

Correspondence to: K. A. Mork (kjell.arne.mork@imr.no)

Published by Copernicus Publications on behalf of the European Geosciences Union.

Abstract

The Norwegian Atlantic Current (NwAC) is the main part of Atlantic water (AW) towards the Arctic. Fluxes of volume, heat and freshwater in the NwAC are estimated for the period 1992–2007 by combining data from a repeated hydrographic transect in the Norwegian Sea with a recently available data set of absolute topography. The analysis shows a two-branch structure of the NwAC in the section, and the calculated absolute velocities are basically in accordance with independent current measurements. Compared with previous estimated fluxes of volume and heat the estimates in the eastern branch (3.7 Sv/118 TW, Sv=10^6 m^3 s^{-1}, TW=10^{12} W) are comparable, the estimates for the western branch (1.4 Sv/39 TW) are lower, partly because of a region with recirculation that previously has been neglected. The total fluxes are lower than the upstream fluxes, but several processes, which are addressed, make the upstream-downstream comparison problematic. The heat flux has positive trend of 4.7 TW yr^{-1} and the freshwater flux has negative trend of −2.4 m Sv yr^{-1}. The trends are results of both increased volume flux (0.13 Sv yr^{-1}) and warmer and saltier inflowing AW. The wind stress curl, spatially averaged over the Norwegian Basin, is on inter-annual scale correlated with both the total fluxes and the occupied area of AW in the section. The latter is influenced by upstream changes in the North Atlantic subpolar gyre on longer time-scale. A first exploitation of the results suggests that increased Atlantic inflow leads to decreased upper ocean stability and delayed phytoplankton spring bloom in the Norwegian Sea, one year later.

1 Introduction

The oceanic fluxes of heat and salt in the NwAC toward the Arctic is of great importance for the climate and ecosystem (Skjoldal, 2004) of the northern region as well as the formation of the returning dense water that takes part in the overturning circulation (Helland-Hansen and Nansen, 1909; Eldevik et al., 2009; Søiland et al., 2008).

OSD

6, 2357–2388, 2009

CC BY

Attempts to monitor the properties of the NwAC go back about a hundred year (e.g. Helland-Hansen and Nansen, 1909; Bochkov, 1982). From about the mid 1950ies several sections have been routinely operated by especially Nordic Fisheries institutions. Since the mid 1990ies arrays of current meter moorings have been operated at the borders and within the Norwegian Sea, providing more quantitative estimates of the fluxes, both mean values and their variability (e.g. Orvik et al., 2001; Ingvaldsen et al., 2004; Østerhus et al., 2005).

Similar variability of hydrographic properties, including a time lag is observed in these arrays (Furevik, 2001; Skagseth et al., 2008; Holliday et al., 2008). The variability of the fluxes are however more questionable. So far there has been little success in comparing the fluxes along-stream the NwAC from the Greenland Scotland Ridge, to the Svinøy section, and further downstream to the Fram Strait and the Barents Sea. Based on the lack of relation between these flux series one cannot simply conclude that the measurements are wrong, since there can be recirculation between the monitoring arrays, and the pathways of the current might vary.

The NwAC manifests itself as a two-branch system in the Norwegian Sea: a western baroclinic jet stream linked to the Arctic Front and an eastern topographic-trapped barotropic current (Fig. 1, e.g. Poulain et al., 1996; Orvik and Niiler, 2002). From long-term current measurements, the variability and forcing of the eastern branch, the Norwegian Atlantic Slope Current (NwASC), has been found to show strong links with both local wind field (Gordon and Huthnance, 1987; Skagseth and Orvik, 2002) and large-scale wind field (Orvik et al., 2001; Orvik and Skagseth, 2003; Skagseth et al., 2004). In contrast, little is known about the variability and forcing of the western branch, herein proposably denoted the Norwegian Atlantic Front Current (NwAFC).

The attempt to estimate absolute fluxes from hydrographic observations is intrinsically linked to the problem of defining a reference level of known motion. In a recent work Hunegnaw et al. (2009) estimated the mean dynamic topography (MDT) for the Nordic Seas by combining the long-wavelength structure of gravity data from the Gravity Recovery and Climate Experiment (GRACE) satellites with the shorter-wavelength ship and airborne surface gravity data along survey lines. The gaps between the surveys lines were then estimated using an iterative combination method (Hipkin and Hunegnaw, 2006). The final MDT was then combined with historical hydrographic data to provide time-averaged volume and heat fluxes in several hydrographic sections. The estimated fluxes were generally in good agreement with fluxes calculated from current measurements.

In this study recently available satellite derived absolute dynamic height data set are combined with repeated hydrographic data from the Svinøy section (Fig. 1), in order to calculate the absolute velocity field and fluxes normal to the section. This includes both long-term averages and variability. Section 2 gives an overview of the data and method. The results, including error estimates, are described in Sect. 3. In Sect. 4, the results are compared with previous published flux estimates and current measurements. Flux variability and extent of AW are in addition related to forcing mechanisms. An effect of the inter-annual flux variability on the ecosystem in the Norwegian Sea is noted at the end of Sect. 4. The conclusion is in Sect. 5.

2 Methods and data

Assuming that the water column is hydrostatic and in geostrophic balance, the geostrophic velocity through the section has a surface (v_s) and a subsurface part (v_{bc})

$$v_g = v_s + v_{bc} \tag{1}$$

with

$$v_{bc} = \frac{g}{\rho_0 f}\int_z^0 \frac{\partial \rho}{\partial x} dz. \tag{2}$$

The x- and y-axes are directed across and along isobaths, respectively, f is the Coriolis parameter, g is the acceleration of gravity, ρ is the density and ρ_0 is a reference

CC BY

density. The surface velocities are given from the altimeter data while the density derived subsurface velocities (Eq. 2) are calculated from hydrographic observations in the section.

Fluxes of volume, heat and freshwater are calculated by area integrating the absolute geostrophic velocity. The heat and freshwater fluxes are calculated relative to a reference temperature (T_{ref}) and salinity (S_{ref})

$$H = \int_A \rho_0 c_p (T - T_{\text{ref}}) v_g dA \tag{3}$$

$$F = -\int_A \rho_0 \frac{(S - S_{\text{ref}})}{S_{\text{ref}}} v_g dA, \tag{4}$$

where c_p is the heat capacity. The reference temperature is set to 0°C, which equals approximately the temperature of the outflow (Østerhus et al., 2005) and also makes a comparison with Østerhus et al. (2005) possible. The reference salinity is set to 34.93, which is used by others in the Nordic Seas (e.g. Aagard and Carmack, 1989; Jónsson, 2007). The vertical flux integration is done both from the surface to the bottom and over the area with water occupied by the northward inflowing AW that is the main focus herein. Here, Atlantic water is defined as water with salinities above 35.0 (e.g. Helland-Hansen and Nansen, 1909).

The Svinøy section with 17 fixed hydrographic stations runs northwestward from the Norwegian coast at about 62° N, 5° E to about 65° N, 0° E (Fig. 1). The section has typically been occupied 4–5 times a year and a total of 82 times during 1992–2007 with simultaneous satellite altimetry. Between pairs of stations sub-surface velocities are calculated from Eq. (2). The flux estimates for the two branches, the NwAFC and the NwASC, are calculated respective offshore and inshore of the 1000 m isobath (see Fig. 1).

The surface velocities are obtained from the AVISO Collecte Localisation Satellites (CLSs) absolute geostrophic velocity data set. The velocities are geostrophic computed from absolute dynamic topography, which are sum of sea level anomaly (SLA) and MDT. The SLA data are based on the merged TOPEX/POSEIDON and ERS-1 and 2 data sets (Ducet et al., 2000), and are corrected for the inverted barometer effect, tides, and dry tropospheric effects (LeTraon and Ogor, 1998). The MDT data (Rio05 data set; Rio and Hernandez, 2004) are based on the GRACE mission, altimetry and in-situ data (hydrography and drifters). The geostrophic surface velocity data set are provided as weekly means with a 1/3° Mercator projection grid. At the Svinøy section (~63° N) this corresponds to a resolution of 17 km. The used period herein ranges from 1992 to 2007. The surface velocity data were interpolated both in time and at the positions between the fixed hydrographic stations to fit with the calculated sub surface velocities. The sum of these two makes the absolute geostrophic velocities through the section (Eq. 1).

Other available current meter and Acoustic Doppler Current Profiler (ADCP) data at 100 m depth, in and near the section, have in addition been used for validation. The current meter data are from the Svinøy section programme (Orvik et al., 2001, ref OSM) while the ADCP data are from the Norwegian Deep Water Programme (Lønseth et al., 2003, see Fig. 1 for locations). Since some of the current measurements are not located at (but still near) the section, the component of the current directed along the isobaths were used for comparison. At the Svinøy section this is approximately similar to the component normal on the section. Table 1 lists the different time periods and locations of the current measurements.

3 Analysis

3.1 Results

The surface velocity data, interpolated on the Svinøy section, is presented as a Hovmöller plot (Fig. 2). Clear features are; the about 50 km wide NwASC centered over the 500 m isobaths, a band of weak but mainly negative velocities (i.e. directed

OSD

6, 2357–2388, 2009

Volume, heat, and freshwater fluxes towards the Arctic

K. A. Mork and Ø. Skagseth

CC BY

toward southwest) over depths of about 1000–1500 m, and again positive velocities in the western part of the order 10 cm/s. This is the region of the NwAFC and the width is similar as for the NwASC, but there are positive values extending west of the Svinøy section. A consistent annual cycle is prominent in the NwASC core velocities showing winter maximum of 30 cm/s and minimum in summer of 20 cm/s (Fig. 3). The seasonal cycle to the west of the NwASC is minor.

The hydrographic conditions and absolute geostrophic velocities in the section for the upper 1000 m are presented as winter and summer averages (Fig. 4). Basically the data show a remarkable stable intercept of AW with the continental slope at 500 m that extend westward as a wedge shaped feature. The main seasonal change is the more homogeneous AW during winter as compared to summer when also a warm and fresh surface layer develops. Below the AW the changes are small. The associated horizontal changes in density show a general increase toward west, but with a local opposite decreasing trend from the hydrographic stations 8 to 5. Associated with the changes in temperature and salinity the upper layer densities are relatively homogeneous during winter as compared to summer where a thin stable layer is prominent. For both season three different velocity regions are clear (Fig. 4, lower figures); the NwASC just off the continental shelf break, the region of weak return current, and finally a western region associated with the NwAFC. The most pronounced seasonal changes are during winter with an anomalous strong NwASC, which extends relatively deep, and also with relatively strong core velocities in the NwAFC. In addition, the return current is less prominent during winter than summer.

Between each pair of hydrographic stations depth integrated fluxes of volume, heat and fresh water are estimated (Fig. 5). The total volume flux, integrated from surface to bottom, have a maximum in the NwASC, then an interior field of negative values, and then again northeastward transports in the region of the NwAFC. The transports are at maximum for winter in both NwASC and NwAFC. When considering only AW the winter maximum in the NwAFC nearly vanishes, but the signature of low values during summer throughout the section prevails. For the heat and freshwater flux the main contribution stem from the NwASC, a minor contribution associated with the NwAFC, and a region of negative fluxes in between these branches. Considering the two branches of the Atlantic inflow, there is a substantial seasonality in the NwASC with winter maximum and summer minimum, and no marked seasonal cycle for the NwAFC (Fig. 5).

In term of volume transport of AW inter-annual variability is seen, but the locations of the two branches appear stable (Fig. 6). Variations in depth of AW are most prominent westward of the NwASC. In the case of anomalous depths in the NwASC they appear with opposite sign in the western branch (see years 1994, 2002, and 2006), but apparently there are no strong relations between the AW depths in the NwASC and the NwAFC.

The AW fluxes of heat, volume, and freshwater show relatively large variability on inter-annual time-scale and large co-variation, and all show significant trends (Fig. 7a). Relative maxima are found in 1995, 1999–2000 and 2005. For the total volume flux the variability is substantially larger, indicating that the deep currents also have a relative large variability. Considering the two branches the overall correlation between the volume flux of the NwASC and the NwAFC is weak (Fig. 7b). After about 2001, however, these branches appear in opposite phase, but this relation does not hold prior to this period. For the NwASC there is a period of remarkable constant and relatively minimum fluxes, about 3 Sv, from 1995 to 1998. The explanation for this is that even though the transports in the core of the NwASC increase during this time, the width of the branch remain anomalous narrow (see Fig. 6). The long-term averaged fluxes with error estimates and trends are summarized in Table 2.

3.2 Error estimates

The uncertainty of the estimates can arise from both the hydrographic data and the satellite sea surface height data. However, the errors in hydrographic data (i.e. density) are typically small compared to the annual mean standard deviation of 0.7 Sv and 20 TW for volume and heat flux, respectively (Table 2). To assess the uncertainty

CC BY

related to the absolute dynamic height data set a comparison with independent current measurements from moorings were made. The comparison shows that even though the absolute values of the observed currents exceed the altimeter current, probably due to smoothing, the structures with the NwASC, the region of counter-current, and the NwAFC appear prominent in both estimates (Fig. 8). This region of counter-current has also been observed with surface drifters (see e.g. Poulain et al., 2006; Orvik and Niiler, 2002).

When using 34.95 instead of 35 as lower salinity limit in the definition of AW, the total averaged volume and heat fluxes increase with 0.4 Sv and 7 TW, respectively. This has however little effect on the variability because of minor changes in the integrated area (see Fig. 4 or e.g. Mork and Blindheim, 2003). An underestimation of the fluxes is that the section might not cover the entire inflow. At the most western station the averaged depth integrated volume and heat fluxes are 0.005 Sv/km and 0.15 TW/km (see Fig. 5). Using these values with 100 km westward extension of the section, to bottom depth larger than 3000 m, gives additional 0.5 Sv and 15 TW for volume and heat flux, respectively.

4 Discussion

In this part, we first compare the mean spatial structure and estimated fluxes of the NwAC with other previous studies. The variability and forcing at seasonal and inter-annual scales are then investigated and the forcing mechanisms are discussed. At final, as a first exploitation of the results, we investigate the effect of the estimated fluxes on large-scale changes in hydrography and phytoplankton production in the Norwegian Sea.

OSD

6, 2357–2388, 2009

4.1 Mean structure and flux estimates

The estimated inflow of AW through the Svinøy section illustrates the two northward branches, both about 50 km wide with maximum averaged velocities of 25 cm/s and about 10 cm/s in the eastern and western branch, respectively. Between these two branches a weak flow in opposite direction is revealed (e.g. Fig. 4). Consistent with our findings, Orvik et al. (2001) observed two 30–50 km wide branches with recirculation in between. However, their observed velocity maxima in the two branches were higher; 30 cm/s in the NwASC based on several years with current measurement, and 14.5 cm/s in the NwAFC based on one-year current meter record. The lower maximum core velocities of this study might be a result of a relatively coarse resolution of the data and due to smoothing effect from gridding of the altimeter data. Nilsen and Nilsen (2007) showed that the topographic locking of the NwAFC depends on the frequency of the wind. This could explain the inter-annual variations in the position of the NwAFC (Fig. 2).

In the NwASC, the estimated fluxes of volume and heat fluxes for this study (3.7 Sv and 118 TW) are comparable to the estimates of Skagseth et al. (2008) based on current meters (4.3 Sv and 126 TW) when considering the error bars (Table 2). Hunegnaw et al. (2009) estimated the NwASC volume flux to 3.9 Sv, and to 4.3 Sv when integrated further westward to 2.8 $^{\circ}$E (near station 6). Upstream in the Faroe-Shetland channel Østerhus et al. (2005) measured the net northward volume and heat fluxes during 1999–2001 to 3.8 Sv and 156 TW, respectively. When averaging over similar observation period (1999–2001) we got slightly larger fluxes (3.8 Sv and 123 TW), compared to the long term averages, which also corresponds well with the estimates in the Faroe-Shetland Channel. This comparison, however, is problematic, because of a significant part of Faroe Current that flows into the Faroe-Shetland channel, and merges with the current there (e.g. Hughes et al., 2006).

Previous volume flux estimates of the NwAFC range from 2.5 Sv to 4.1 Sv (Mork and Blindheim, 2000; Orvik et al., 2001), significant larger than our estimate of 1.4 Sv.

OSD
6, 2357–2388, 2009

CC BY

These estimate, however, are either based on hydrographic calculations, depending heavily on a level of no (or known) motion (Mork and Blindheim, 2000; Orvik et al., 2001), or some few snapshots from ship ADCP-measurements (Orvik et al., 2001). A comparison is therefore done with observations in the Faroe Current, which is regarded upstream of the NwAFC (e.g. Poulain et al., 1996; Orvik and Niiler, 2002). Østerhus et al. (2005) estimated the volume and heat fluxes in the Faroe Current during 1999–2001 to 3.8 Sv and 134 TW, respectively, while Hunegnaw (2009) calculated the fluxes of the Faroe Current to 2.9 Sv and 78 TW. Hughes et al. (2006) estimated that 1.7 Sv and 70 TW leave this current northeast of Faroe, and flow southward into the Faroe-Shetland Channel (see Fig. 1). When subtracting these fluxes from the estimates of Østerhus et al. (2005) the relevant fluxes for comparison of the NwAFC are 2.1 Sv and 64 TW. The estimated volume and heat flux estimates in the NwAFC in this study are 1.4 Sv and 39 TW, and for the years 1999–2001 the estimates are 1.8 Sv and 49 TW. When considering modification enroute the current from the Faroe to the Svinøy section, a distance of the order 400 km, with e.g. cooling and frontal instabilities, these differences in fluxes, 0.3 Sv and 15 TW, are small and also within the error estimates. Rossby et al. (2009) reported that the majority of drifters deployed at 200 m depth in the Faroe Current crossed over to the NwASC. This indicates that considerable exchange takes place between the two branches of the NwAC upstream of the Svinøy section, thus complicating comparison of flux estimates along stream the NwAC.

The total fluxes of volume and heat over the Greenland-Scotland Ridge for the period 1999–2001 was 8.5 Sv and 313 TW (Østerhus et al., 2005). Of these about 0.8 Sv and 22 TW are contribution from the North Icelandic Irminger Current and are not likely to reach the southern Norwegian Sea, and thus the relevant fluxes for comparison are 7.7 Sv and 291 TW. Here, the estimated long-term mean total fluxes of volume and heat for similar period are 5.6 Sv and 173 TW, respectively. Furthermore, there is also the Norwegian Coastal Current (NCC) that carries 0.8 Sv (based on data from Blindheim, 1989). When assuming there is also a contribution of ∼0.5 Sv northwest and outside our section, commented in Sect. 3.2, the total northward flux for comparison is 6.9 Sv. This is somewhat less (0.8 Sv) compared to Østerhus et al. (2005), but not significantly different when considering the associated errors.

4.2 Variability and forcing

Previous studies have identified the along-slope component of the wind to be the main forcing of the variability in the NwASC with a minor time lag, thus indicating a strong barotropic mechanism (Skagseth and Orvik, 2002; Skagseth et al., 2004). In accordance with this, our estimated volume flux in NwASC shows a similar relation to the along-slope component of the wind (not shown). The general stronger wind forcing during winter explains the seasonal variation in the NwASC (Fig. 9). Minimum volume flux is 2.3 Sv in July–September, while maximum is 4.9 Sv in December–February. The deep circulation within closed isobaths in the Norwegian Sea and Nordic Seas are found to be largely influenced by the wind stress curl, averaged within the isobaths (e.g. Isachsen et al, 2003; Mork and Skagseth, 2005; Nøst and Isachsen, 2005), with largest bottom velocity in March and lowest in August (Mork and Skagseth, 2005). The estimated volume flux in the NwAFC has a weaker seasonal signal than in the NwASC (Fig. 9). Comparable with Mork and Skagseth (2005) minimum and maximum volume flux is during August (1 Sv) and February (2 Sv), respectively.

On inter-annual time scales the averaged wind stress curl over the Norwegian Basin is significantly correlated with the total volume flux for AW, and also with the heat and freshwater fluxes due to their close relation with the volume flux (r=0.6 for the volume and heat fluxes and −0.6 for the freshwater flux, significant at 95% level). For the individual branches no significant relation to the wind stress curl is found. Instead, when the depth integrated volume flux at each station pair was correlated with the wind stress curl maximum correlation (significant at 95% level) was found for the stations in the middle of the section, i.e. between the two branches.

Based on hydrographic data Mork and Blindheim (2000) reported that the two branches in the Svinøy section fluctuated in opposite phase. Nilsen et al. (2003) found negative correlation between the inflow fluxes in the Faroe and Shetland branch using

OSD
6, 2357–2388, 2009

a numerical model. Østerhus et al. (2008) indicated a similar relationship, but the time series were too short for being significant. The results herein show that the branches appear to be in opposite phase after 2001 (see Fig. 7), but that there is no overall significant correlation between the two branches.

Holliday et al. (2008) reported that since the 1990s both temperature and salinity have increased in the Atlantic inflow. The fluxes of volume, heat, and freshwater, have all significant trends, and the trends in the heat and freshwater fluxes are thus a result of both increased volume flux and warmer and saltier inflowing AW.

The inter-annual variability in the area of AW is, for the NwAFC, strongly influenced by the averaged wind stress curl over the Norwegian Basin (Fig. 10). Using yearly averages (13 data points) the correlation coefficient between the two is −0.72 (>99% significant) while using monthly values resulted in correlation of $r=-0.60$ (>95% significant). In the NwASC the variability in the area of AW is small. Thus an increased (decreased) wind stress curl leads to less (more) AW in the section. Mork and Blindheim (2000) and Blindheim et al. (2000) came to similar conclusion using the NAO index. The wind stress curl has only a minor positive trend and cannot explain the trend of increased area of AW in the NwAFC. Another forcing mechanism is the strength of the sub-polar gyre in the North Atlantic that affects the properties of the inflowing Atlantic Water to the Norwegian Sea. Decreased (increased) strength of the sub-polar gyre results in a westward (eastward) movement of the sub-polar front, which allows more (less) of the warmer and saline Eastern North Atlantic Water to enter the Norwegian Sea (e.g. Hakkinen and Rhines, 2004; Hathun et al., 2005). The positive trend in area of AW is likely due to a reduced strength of the sub-polar gyre (Fig. 10). This suggests that the area of AW in the Svinøy section is determined by the basin averaged wind stress curl on inter-annual time-scales, whereas the trend is related to changes in the upstream condition connected to the sub-polar gyre changes.

4.3 Impact on the ecosystem

The fluxes impact the ocean climate and thus the ecosystem for the region. As a first exploitation of the results the fluxes are compared with some key parameters in the Norwegian Sea ecosystem.

Melle et al. (2009) revealed relationships from upper ocean stability to the onset of the phytoplankton spring bloom, zooplankton biomass, and herring growth in the Norwegian Sea based on yearly synoptic ecosystem surveys. For the Norwegian Sea, the phytoplankton spring bloom in AW is dependent on the stabilizing process of the water column, which leads to a shallow thermocline (Rey, 2004). Extending on this, the annually averaged total volume flux of AW in the Svinøy section is compared with the stability of the water column in the Norwegian Sea and the timing of the phytoplankton bloom (Fig. 11).

Maximum correlation ($r=-0.71$, >99% significant) is found for the volume flux leading the upper layer stability in the Norwegian Sea by nearly 1.5 year. Similar, the volume flux also leads the timing of bloom with nearly 1.5 year ($r=0.67$, >95% significant). Thus, on inter-annual time-scales there is a negative effect of the Atlantic inflow on the ecosystem through warming of the sub-surface layers leading to reduced stability and a subsequent delay of the phytoplankton spring bloom. This is not to say that the inflow of Atlantic water in general is negative for the ecosystems, but points out a possible opposite effect to consider on inter-annual time-scale. Comparable to the 1.5 year time lag is that both Skagseth et al. (2008) and Holliday et al. (2008) estimated that the variability in the hydrographic properties are observed two years later in the northern Norwegian Sea compared to the observed variability in the southern Norwegian Sea.

cc BY

5 Concluding remarks

We have presented a method to calculate fluxes of volume, heat, and freshwater using a combination of altimetry and repeated hydrographic data in a section. The method is general, but we have used it to calculate the northward fluxes in the Svinøy section, located in the southern Norwegian Sea, because of the extensive hydrographic data and available current measurements there. Based on this method, the resulting currents have shown to agree well with the available independent current meter data, giving general confidence in the results.

The total inflow is significantly lower compared to downstream fluxes over the Greenland-Scotland Ridge, but recirculation and frontal instabilities together with other sub-branches, such as the NCC, makes the downstream and upstream flows not easily comparable. The volume and heat fluxes have positive trends, the freshwater flux has negative trend during the observation period, 1993–2007. Largest trends are for the western branch, the NwAFC.

The averaged wind stress curl over the Norwegian Basin is significantly correlated with both the total volume flux of AW and the area of occupied AW in the section. The positive trend for the latter is likely as a result of the reduced strength in the North Atlantic sub-polar gyre. In contrast to the general view that increased inflow of Atlantic water is beneficial for the Norwegian Sea ecosystem, our results suggests a negative relation on inter-annual time scale; increased Atlantic inflow leads to a reduced stability of the water column and delayed phytoplankton spring bloom. The time lag of nearly 1.5 years, where the volume flux leads, gives a potential for ecosystem predictions.

Acknowledgements. This work has been funded by the Norwegian Research Council through the POCAHONTAS project. We are grateful to Tor Eldevik for his comments. Current measurements from the Norwegian Deep Water programmed were kindly made available by H. J. Sætre. The altimeter products, produced by SSALTO/DUACS, were obtained from AVISO http://www.aviso.oceanobs.com/

CC BY

References

Aagard, K. and Carmack, E.C.: The role of sea ice and other fresh water in the Arctic circulation, J. Geophys. Res., 94, 14485–14498, 1989.

Blindheim, J.: Cascading of Barents Sea bottom water into the Norwegian Sea, Rapp. P.-v. Réun. Cons. Int. Explor. Mer, 188, 49–58, 1989.

Blindheim, J., Borovkov, V., Hansen, B., Malmberg, S. Aa., Turrell, W. R., and Østerhus, S.: Upper layer cooling and freshening in the Norwegian Sea in relation to atmospheric forcing, Deep-Sea Res., 47, 655–680, 2000.

Bochkov, Y. A.: Water temperature in the 0–200 m layer in the Kola-Meridian section in the Barents Sea, 1900–1981, Sb. Nauchn. Trud. PINRO, 46, 113–122, 1982 (in Russian).

Ducet, N., LeTraon, P. Y., and Reverdin, G.: Global high-resolution mapping of ocean circulation from TOPEX/Poseidon and ERS-1 and 2, J. Geophys. Res., 105, 19477–19498, 2000.

Eldevik, T., Nilsen, J. E. Ø., Iovino, D., Olsson, K. A., Sandø, A. B., and Drange, H.: Observed sources and variability of Nordic seas overflow, Nature Geosci., 2, 405–409, doi:10.1038/NGEO518, 2009.

Furevik, T.: Annual and interannual variability of the Atlantic water temperatures in the Norwegian and Barents seas: 1980–1996, Deep-Sea Res. I, 48, 383–404, 2001.

Gordon, R. L. and Huthnance, J.: Storm-driven continental shelf waves over the Scottish continental shelf, Cont. Shelf Res., 7, 1015–1048, 1987.

Häkkinen, S. and Rhines, P. B.: Decline of Subpolar North Atlantic Circulation During the 1990s, Science, 304, 555–559, 2004.

Hátún, H., Sandø, A. B., Drange, H., Hansen, B., and Valdimarsson, H.: Influence of the Atlantic Subpolar Gyre on the Thermohaline Circulation, Science, 309, 1841–1844, doi:10.1126/Science.1114777, 2005.

Helland-Hansen, B. and Nansen, F.: The Norwegian Sea. Its physical oceanography based upon the Norwegian Researches 1900–1904, Report on Norwegian Fishery and Marine Investigations, 2(2), 1–360, 1909.

Hipkin, R. and Hunegnaw, A.: Mean dynamic topography by an iterative combination method, in: Proceedings of the Workshop on GOCINA: Improving Modelling of Ocean Transport and climate Prediction in the North Atlantic Region Using GOCE Gravimetry, edited by: Knudsen, P., Johannessen J., Gruber T., Stammer S., and van Dam T., Cah. Cent. Eur. Geodyn. Seismol., 25, 11–16, 2006.

Holliday, P., Hughes, S. L., Bacon, S., Beszczynska-Möller, A., Hansen, B., Lavín, A., Loeng, H., Mork, K. A., Østerhus, S., Sherwin, T., and Walczowski, W.: Reversal of the 1960s–1990s Freshening Trend in the North Atlantic and Nordic Seas, Geophys. Res. Lett., 35, L03614, doi:10.1029/2007GL032675, 2008.
Hughes, S. L., Turrell, W. R., and Hansen, B., Østerhus, S.: Fluxes of Atlantic water (volume, heat and salt) in the Faroe-Shetland Channel calculated from a decade of Acoustic Doppler Current Profile data (1994–2005), Fisheries Research Services Collaborative Report No: 01/06, Marine Laboratory, Aberdeen, Scotland, 2006.
Hunegnaw, A., Siegismund, F., Hipkin, R., and Mork, K. A.: Absolute flow field estimation for the Nordic seas from combined gravimetric, altimetric, and in situ data, J. Geophys. Res., 114, C02022, doi:10.1029/2008JC004797, 2009.
Ingvaldsen, R. B., Asplin, L., and Loeng, H.: The seasonal cycle in the Atlantic transport to the Barents Sea during the years 1997–2001, Cont. Shelf. Res., 24, 1015–1032, 2004.
Isachsen, P. E., LaCasce, J. H., Mauritzen, C., and Häkkinen, S.: Wind-driven variability of the large-scale recirculating flow in the Nordic Seas and Arctic Ocean, J. Phys. Ocean., 33, 2534–2550, 2003.
Jónsson, S.: Volume flux and fresh water transport associated with the East Icelandic Current, Prog. Oceanogr., 73, 231–241, 2007.
Le Traon, P. Y. and Ogor, F.: ERS-1/2 orbit improvement using TOPEX/Poseidon: The 2 cm challenge, J. Geophys. Res., 103, 8045–8057, 1998.
Lønseth, L., Eidnes, G., and Mathisen, J. P.: Norwegian Deep Water Measurement Programme 2001–2, OCEANOR report, OCN R-23021, 2003.
Melle, W., Holst, J. C., and Mork, K. A.: Variations in hydrography, zooplankton production and growth of a planktivorous fish in relation to climate variability, in preparation, 2009.
Mork, K. A. and Blindheim, J.: Variations in the Atlantic inflow to the Nordic Seas, 1955–1999, Deep-Sea Res. I, 47, 1035–1057, 2000.
Mork, K. A. and Blindheim, J.: Heat loss of the Norwegian Atlantic Current toward the Arctic, ICES Mar. Sci. Symp., 219, 144–149, 2003.
Mork, K. A. and Skagseth, Ø.: Annual Sea Surface Height Variability in the Nordic Seas, in: The Nordic Seas: An Integrated Perspective, edited by: Drange, H., Dokken T., Furevik, T., Gerdes, R., and Berger, W., Geophys. Monogr. Ser., 158, AGU, Washington, DC, 2005.
Nilsen, J. E. Ø. and Nilsen, F.: The Atlantic Water flow along the Vøring Plateau: Detecting frontal structures in oceanic station time series, Deep-Sea Res. I, 54, 297–319, 2007.

Nilsen, J. E. Ø., Gao, Y., Drange, H., Furevik, T., and Bentsen, M.: Simulated North Atlantic-Nordic Seas water mass exchanges in an isopycnic coordinate OGCM, Geophys. Res. Lett., 30(10), 1536, doi:10.1029/2002GL016597, 2003.

Nøst, O. A. and Isachsen, P. E.: The large-scale time-mean circulation in the Nordic Seas and Arctic Ocean estimated from simplified dynamics, J. Mar. Res., 61, 175–210, 2003.

Orvik, K. A., Skagseth, Ø., and Mork, M.: Atlantic inflow to the Nordic Seas: Current structure and volume fluxes from moored current meters, VM-ADCP and SeaSoar-CTD observations, 1995–1999, Deep-Sea Res. I, 48, 937–957, 2001.

Orvik, K. A. and Niiler, P.: Major pathways of Atlantic water in the northern North Atlantic and Nordic Seas toward Arctic, Geophys. Res. Lett., 29(19), 1896, doi:10.1029/2002GL015002, 2002.

Orvik, K. A. and Skagseth, Ø.: The impact of the wind stress curl in the North Atlantic on the Atlantic inflow to the Norwegian Sea toward the Arctic, Geophys. Res Lett., 30(17), 1884, doi:10.1029/2003GL017932, 2003.

Poulain, P. M., Warn-Varnas, A., and Niiler, P.: Near-surface circulation of the Nordic seas as measured by Lagrangian drifters, J. Geophys. Res., 101, 18237–18258, 1996.

Rey, F.: Phytoplankton: the grass of the sea, in: The Norwegian Sea Ecosystem, edited by: Skoldal, H. R., Tapir Academic Press, Trondheim, Norway, ISBN 82-519-1841-3, 97–136, 2004.

Rio M.-H. and Hernandez, F.: A mean dynamic topography computed over the world ocean from altimetry, in situ measurements, and a geoid model, J. Geophys. Res., 109, C12032, doi:10.1029/2003JC002226, 2004.

Rossby, T., Prater, M., and Søiland, H.: Pathways of inflow and dispersion of warm water in the Nordic Seas, J. Geophys. Res., 114, C04011, doi:10.1029/2008JC005073, 2009.

Skagseth, Ø. and Orvik, K. A.: Identifying fluctuations in the Norwegian Atlantic Slope Current by means of empirical orthogonal functions, Cont. Shelf Res., 22, 547–563, 2002.

Skagseth, Ø., Orvik, K. A., and Furevik, T.: Coherent variability of the Norwegian Atlantic Slope Current derived from TOPEX/ERS altimeter data, Geophys. Res. Lett., 31, L14304, doi:10.1029/2004GL020057, 2004.

Skagseth, Ø., Furevik, T., Ingvaldsen, R., Loeng, H., Mork, K. A., Orvik, K. A., and Ozhigin, V.: Volume and heat transports to the Arctic Ocean via the Norwegian and Barents Seas, in: Arctic-Subarctic Ocean Fluxes: Defining the role of the Northern Seas in Climate, edited by: Dickson, B., Meincke, J., and Rhines, P., Springer Verlag, Nederland, 45–64, 2008.

Skoldal, H. R.: The Norwegian Sea Ecosystem, Tapir Academic Press, ISBN 82-519-1841-3, 559 pp., 2004.
Søiland, H., Prater, M., and Rossby, T.: Rigid topographic control of currents in the Nordic Seas, Geophys. Res. Lett., 35, L18607, doi:10.1029/2008GL034846, 2008.
Østerhus, S., Turrell, W. R., Jónsson, S., and Hansen, B.: Measured volume, heat, and salt fluxes from the Atlantic to the Arctic Mediterranean, Geophys. Res. Lett., 32, L07603, doi:10.1029/2004GL022188, 2005.

OSD
6, 2357–2388, 2009

Volume, heat, and freshwater fluxes towards the Arctic

K. A. Mork and Ø. Skagseth

Table 1. Time periods and locations of the current measurements used for validation. Locations are also shown in Figs. 1 and 8. OSM-instruments, from Orvik et al. (2001), are current meters. NDP-instruments, from the Norwegian Deep Water Programme (Lønseth et al., 2003), are ADCP measurements. All measurements are at 100 m depth.

Instrument	Time period	Position
OSM-1	Apr 1995–Oct 1998	62°48′ N, 4°15′ E
OSM-2	Oct 1995–Oct 1998	62°53′ N, 4°06′ E
OSM-3	Oct 1996–Oct 1998	63°00′ N, 3°53′ E
OSM-4	Apr 1997–Oct 1998	63°11′ N, 3°23′ E
OSM-5	Apr 1997–Oct 1998	63°58′ N, 1°39′ E
NDP-1	Dec 2001–May 2002	63°30′ N, 3°00′ E
NDP-2	Dec 2001–May 2002	64°10′ N, 3°00′ E
NDP-3	Dec 2001–May 2002	64°15′ N, 4°20′ E

OSD

6, 2357–2388, 2009

Table 2. Mean flux estimates for total flux in the section (for both total and only AW), and for the two branches with AW. Error estimates are also included. The error estimates are mean error estimates of annual means ($\sigma_m = \sigma/\sqrt{N-1}$), where σ is the standard deviation for N observations within a year. The numbers in parenthesis are flux averages over the period 1999–2001 for comparison with Østerhus et al. (2005). Trends with significance are calculated for some flux estimates where autocorrelation has been accounted for.

Branch	Volume (Sv)	Heat (TW)	Freshwater (mSv)
Total	6.8±2.1	179±21	−58±14
Total of AW	5.0±0.7 (5.6) 0.13 $Svyr^{-1}$, $p=4\times10^{-3}$	157±21 (173) 4.7 $TWyr^{-1}$, $p=5\times10^{-4}$	−58±8 −2.4 $mSvyr^{-1}$, $p=10^{-4}$
NwASC of AW	3.7±0.6 (3.8) 0.04 $Svyr^{-1}$, $p=0.13$	118±19 (123)	−45±8
NwAFC of AW	1.4±0.4 (1.8) 0.09 $Svyr^{-1}$, $p=0.01$	39±13 (49)	−13±5

OSD
6, 2357–2388, 2009

Volume, heat, and freshwater fluxes towards the Arctic

K. A. Mork and Ø. Skagseth

CC BY

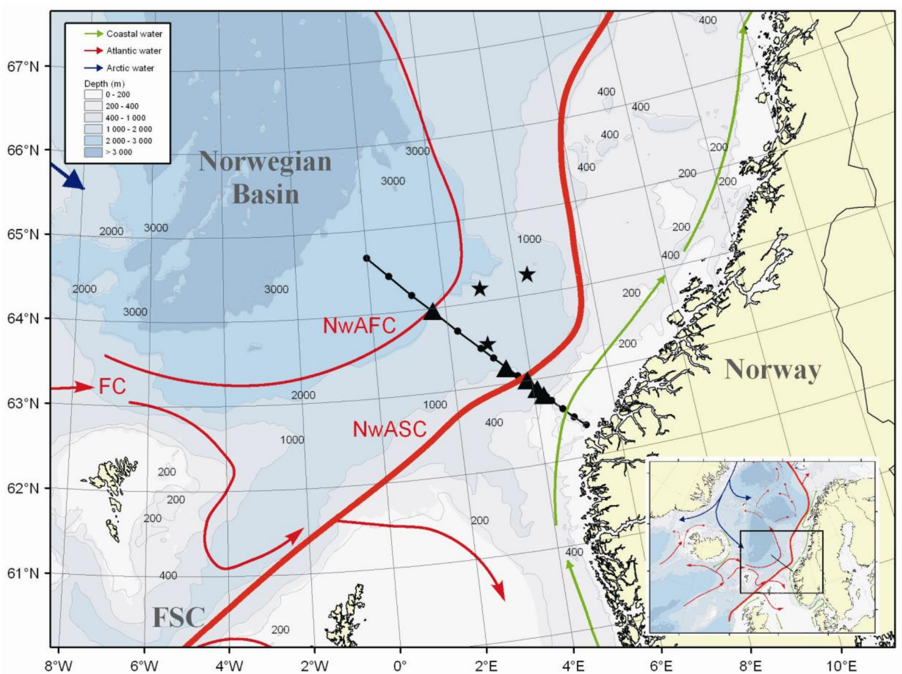

Fig. 1. Map of the study area in the southern Norwegian Sea. The locations of the Svinøy section (black line) with the 17 hydrographic stations (black dots) are shown. The current measurements (OSM: black triangles, NDP: black stars) used for validation are also illustrated. See Table 1 for more details of the current measurements. The Faroe-Shetland Channel (FSC), Faroe current (FC), and the two branches: the Norwegian Atlantic Slope Current (NwASC) and the Norwegian Atlantic Front Current (NwAFC) are also indicated.

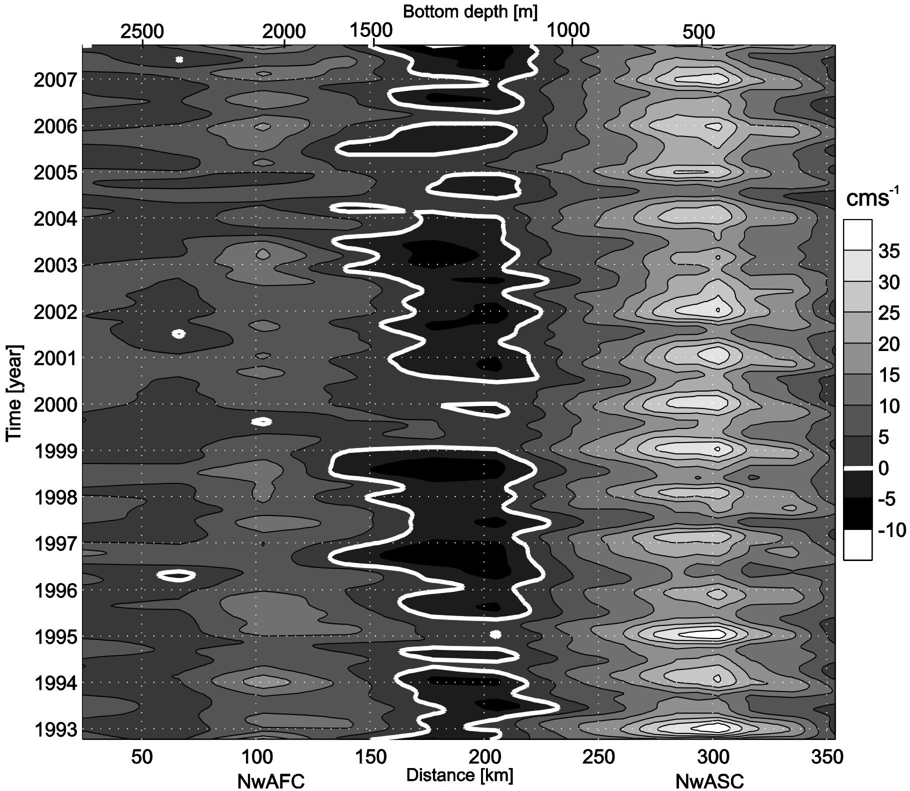

Fig. 2. Hovmöller plot of surface currents (cm s^{-1}) based on the absolute topography satellite data. White contour lines indicate zero velocities. The Norwegian coast is to the right.

OSD

6, 2357–2388, 2009

Volume, heat, and freshwater fluxes towards the Arctic

K. A. Mork and Ø. Skagseth

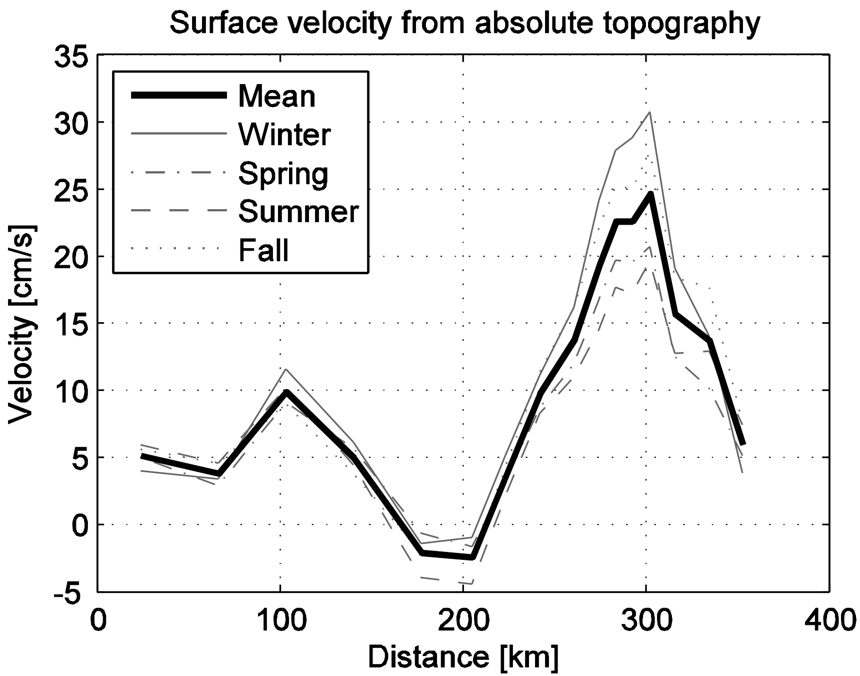

Fig. 3. Mean seasonal averaged surface velocity from absolute topography satellite data in the section.

OSD
6, 2357–2388, 2009

Volume, heat, and freshwater fluxes towards the Arctic

K. A. Mork and Ø. Skagseth

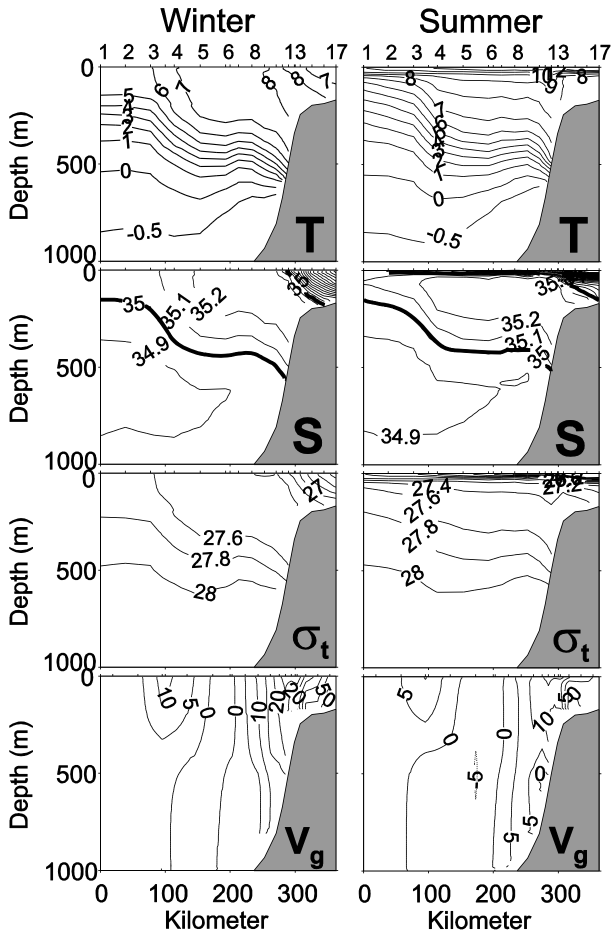

Fig. 4. Cross sections of temperature, salinity, density (sigma-t) and absolute velocity ($cm\,s^{-1}$) averaged for winter and summer.

OSD

6, 2357–2388, 2009

Volume, heat, and freshwater fluxes towards the Arctic

K. A. Mork and Ø. Skagseth

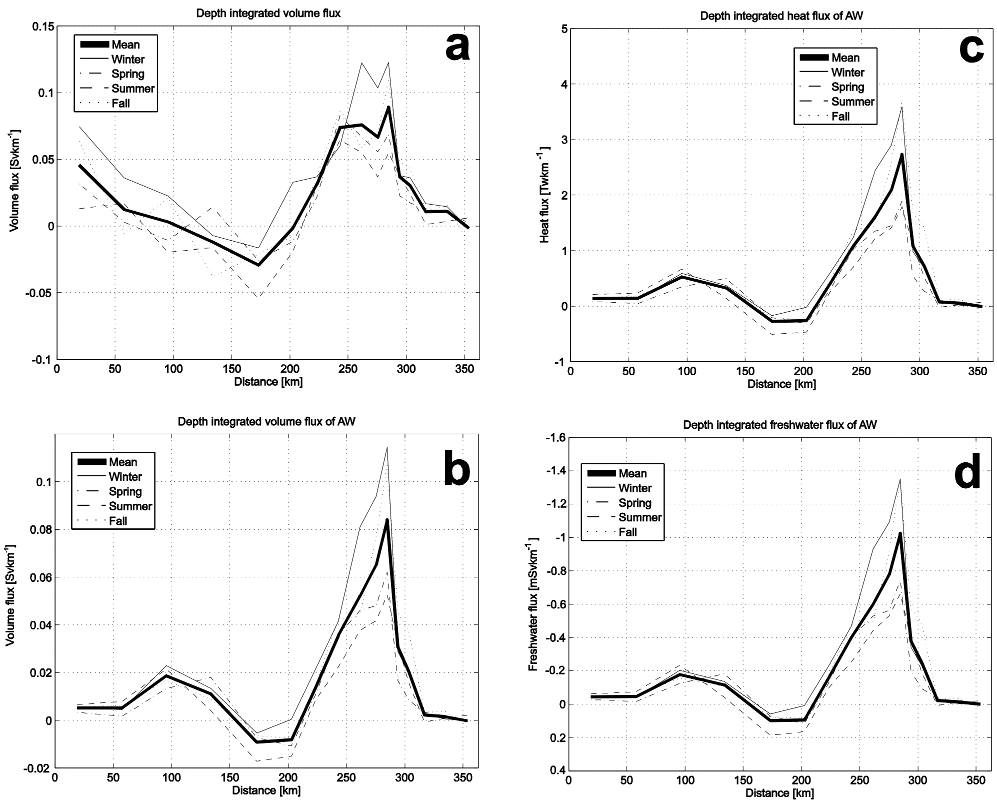

Fig. 5. Seasonal averaged depth integrated fluxes in the Svinøy section; **(a)** total volume flux, **(b)** volume flux of AW, **(c)** heat flux of AW, and **(d)** freshwater flux of AW. Note the different scales of the y-axis.

OSD
6, 2357–2388, 2009

K. A. Mork and Ø. Skagseth

CC BY

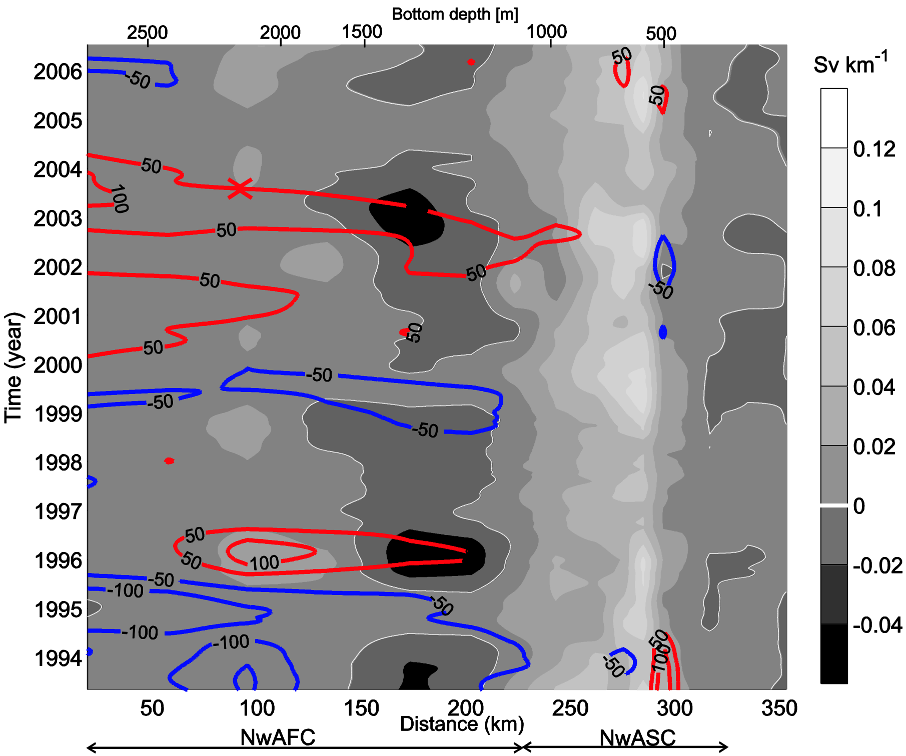

Fig. 6. Hovmöller diagram of vertically depth integrated volume flux of Atlantic Water as function of position in the section and time. Shaded contour interval is 0.02 Sv km^{-1}. White contours indicate zero flux. Red and blue lines are positive and negative anomalies of AW thickness, respectively.

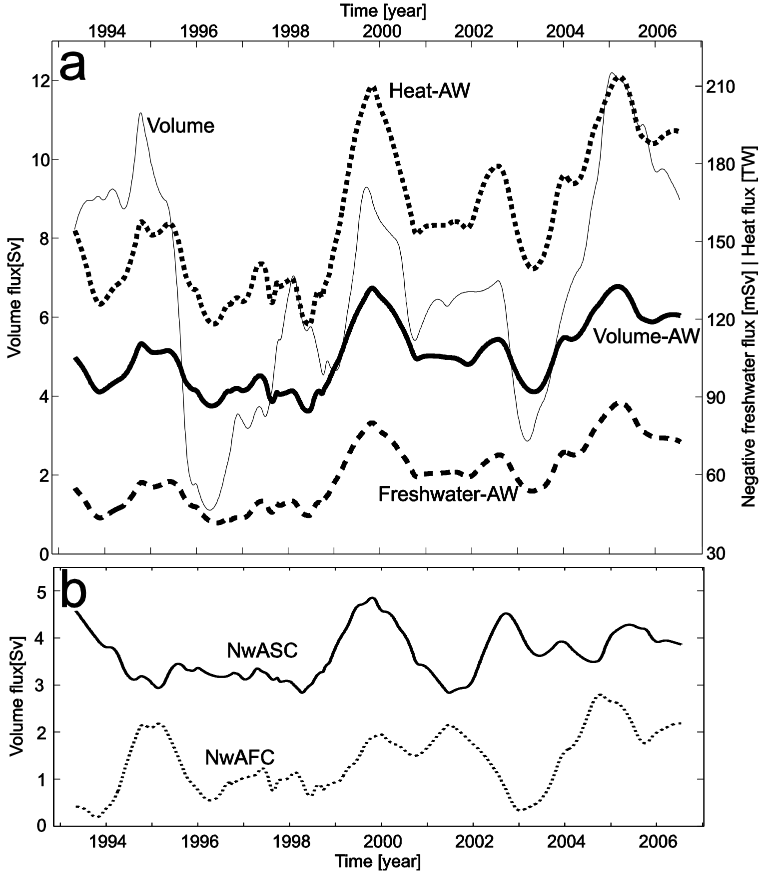

Fig. 7. (a) Time series of total volume, heat, and salt flux for AW, and total volume flux integrated to bottom. The fluxes are integrated over the whole section (i.e. stations 1–15). **(b)** Volume flux of AW for the eastern (NwASC) and western (NwAFC) branch. All time series are one year moving averages.

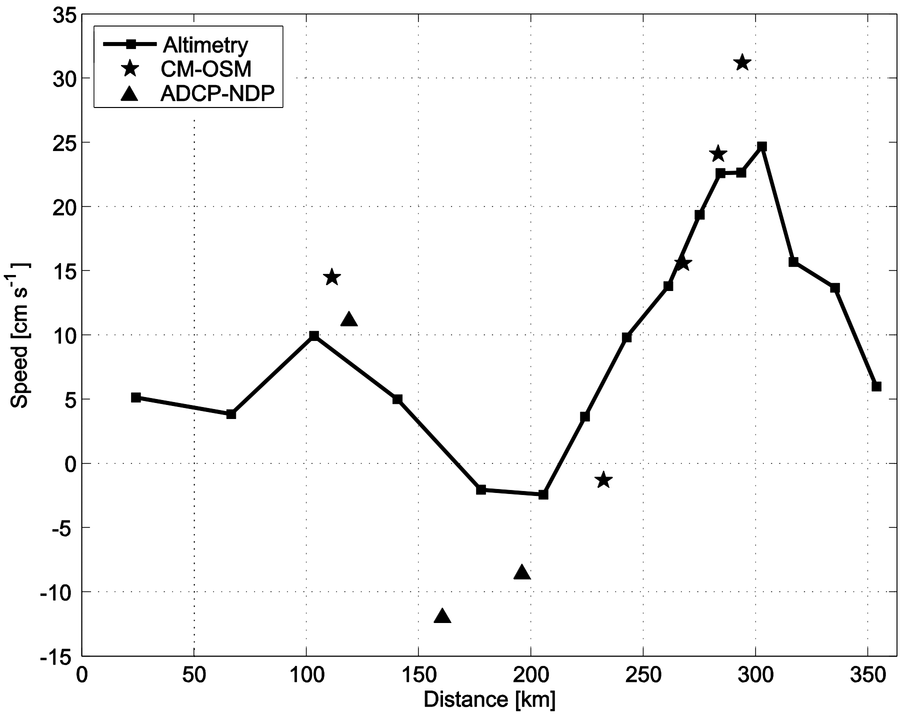

Fig. 8. Mean speed of surface velocity across the Svinøy section from the altimetry data. Speeds, at 100 m depth, from single CMs from Orvik et al. (2001, ref OSM) and ADCPs from the Norwegian Deep Water Current programme (ref NDP) are included.

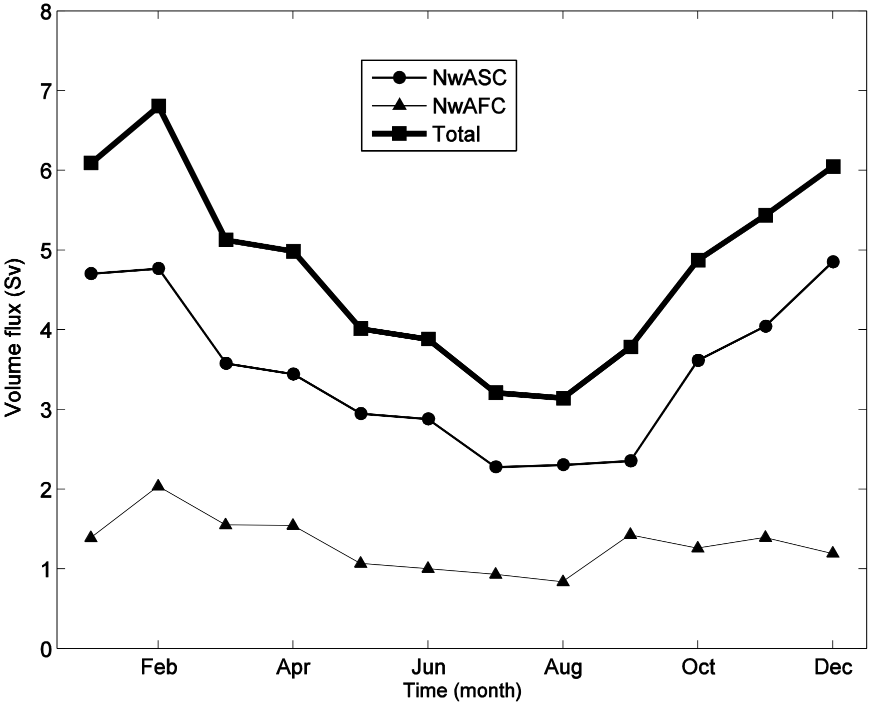

Fig. 9. Monthly values of volume flux in AW, for the two branches NwASC and NwAFC, and for the total.

CC BY

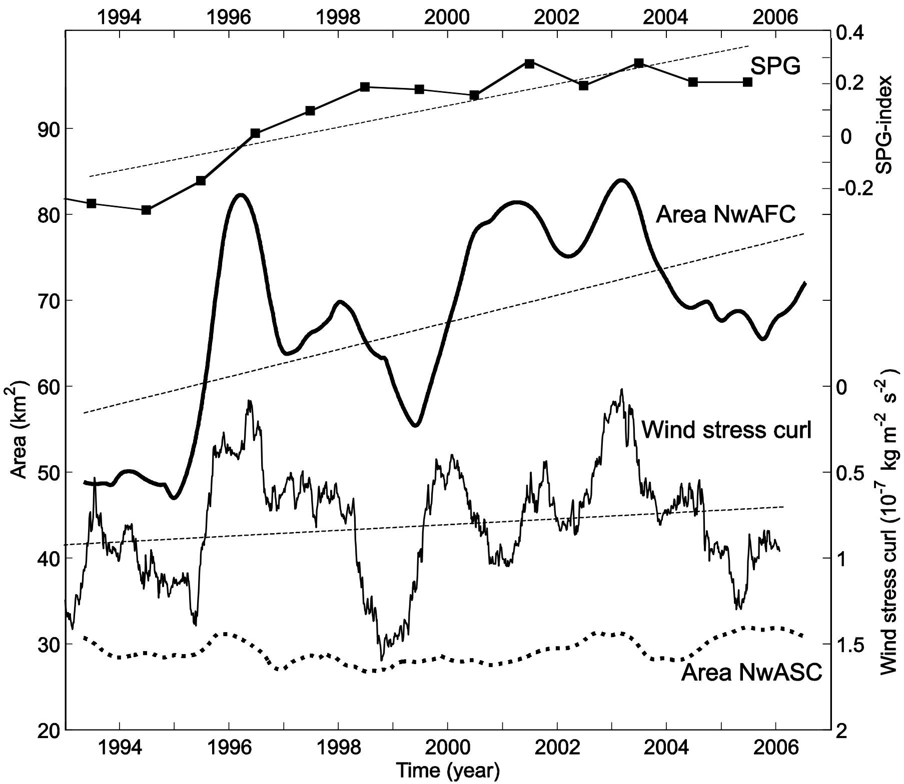

Fig. 10. Area of AW in the two branches, wind stress curl over the Norwegian Basin, and subpolar gyre index. All time series are one year moving averages except the SPG-index that are yearly values. Trends are also indicated. Note that the y-axis for the wind is reversed. The SPG-index is obtained in similar way as in Häkkinen and Rhines (2004).

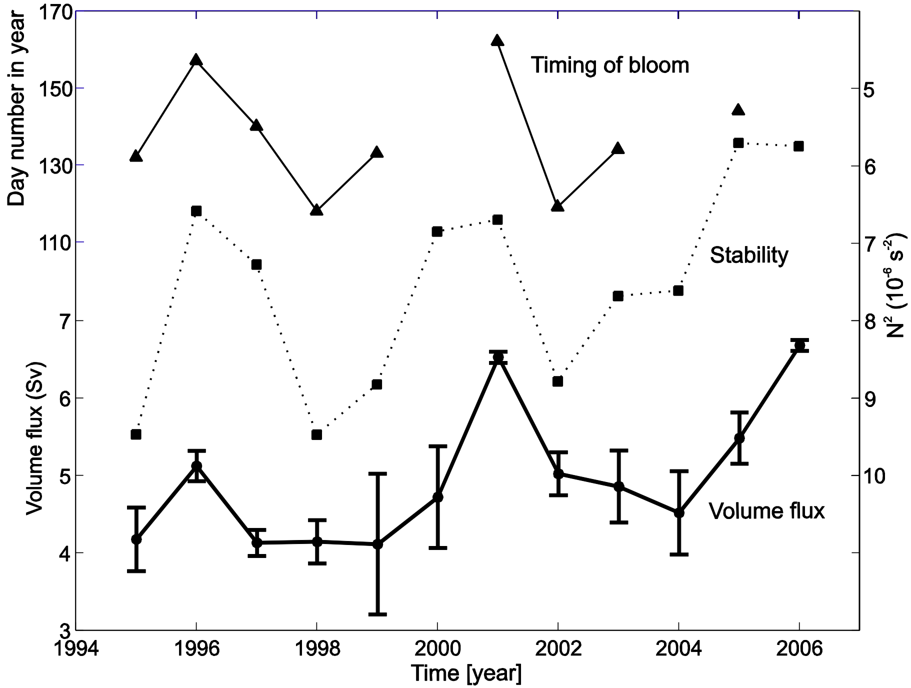

Fig. 11. Time series of volume flux of AW, the stability ($N^2=-\frac{g}{\rho}\frac{\partial\rho}{\partial z}$), and the timing of phytoplankton bloom at Ocean Weather Station M (located at 66° N, 2° E). The volume flux data are averages over one year centered at 1 January the previous year compared to the other two time series. The time series of the volume flux are moved for better visualization. The bars at the volume flux indicate standard deviation within each year. The stability (N^2) is averaged over the upper 200 m, and for only AW in the Norwegian, during end of April to beginning of June. Note that y-axis for stability is reversed. The stability data are from Melle et al. (2009), and the timing of bloom data are from Rey (2004).

OSD

6, 2357–2388, 2009

Volume, heat, and freshwater fluxes towards the Arctic

K. A. Mork and Ø. Skagseth

CC BY